Environ Sci Pollut Res (2016) 23:9585–9597
DOI 10.1007/s11356-016-6164-9

RESEARCH ARTICLE

Degradation and detoxification of the triphenylmethane dye malachite green catalyzed by crude manganese peroxidase from *Irpex lacteus* F17

Xueting Yang[1] · **Jinzhao Zheng**[1] · **Yongming Lu**[1] · **Rong Jia**[1]

Received: 16 October 2015 / Accepted: 21 January 2016 / Published online: 4 February 2016

Abstract Malachite green (MG), a recalcitrant, carcinogenic, and mutagenic triphenylmethane dye, was decolorized and detoxified using crude manganese peroxidase (MnP) prepared from the white rot fungus *Irpex lacteus* F17. In this study, the key factors (pH, temperature, MG, Mn^{2+}, H_2O_2, MnP) in these processes were investigated. Under optimal conditions, 96 % of 200 mg L^{-1} of MG was decolorized when 66.32 U L^{-1} of MnP was added for 1 h. The K_m, V_{max}, and k_{cat} values were 109.9 μmol L^{-1}, 152.8 μmol L^{-1} min^{-1}, and 44.5 s^{-1}, respectively. The decolorization of MG by MnP followed first-order reaction kinetics with a kinetic rate constant of 0.0129 h^{-1}. UV–vis and UPLC analysis revealed degradation of MG. Furthermore, seven different intermediates formed during the MnP treatment of 0.5 h were identified by LC-TOF-MS. These degradation products were generated via two different routes by either *N*-demethylation of MG or the oxidative cleavage of the C–C double bond in MG. Based on ecotoxicity analyses performed on bacteria and algae, it was confirmed that MG metabolites produced by the MnP-catalyzed system were appreciably less toxic than the parent compound. These studies indicate the potential use of this enzyme system in the clean-up of aquatic and terrestrial environments.

Responsible editor: Philippe Garrigues

Electronic supplementary material The online version of this article (doi:10.1007/s11356-016-6164-9) contains supplementary material, which is available to authorized users.

✉ Rong Jia
ahdxjiarong@126.com

[1] School of Life Science, Anhui University, Hefei 230601, People's Republic of China

Keywords Malachite green · Manganese peroxidase · Enzymatic decolorization · Kinetics · Degradation · Ecotoxicity

Introduction

Malachite green (MG), a triphenylmethane dye, is widely used in the silk, wool, jute, cotton, paper, and acrylic industries, and as an ectoparasiticide in the aquaculture industry, as a food additive, and a medical disinfectant (Srivastava et al. 2004). However, this compound has become highly controversial, based on the significant risk it poses to a variety of aquatic and terrestrial animals. Subacute (0.10 mg L^{-1}) and sublethal (0.05 mg L^{-1}) concentrations of MG can cause decrease in serum calcium and protein levels of fishers after only a short-term exposure (10~20 days) (Srivastava et al. 1995) and it is highly toxic to mammalian cells at a concentration as low as 0.1 mg mL^{-1} (Clemmensen et al. 1984). Further, several studies have shown that ingestion of this dye reduces fertility and leads to mutagenic, carcinogenic effects on human and other animals (Chaturvedi et al. 2013). Moreover, MG is environmentally persistent. When released into water bodies, MG can lead to a reduction in sunlight transmission, which in turn decreases both photosynthetic activity and dissolution of oxygen concentration thereby affecting aquatic biota in the habitat (Gokulakrishnan et al. 2012). Therefore, effective removal of MG from water bodies is crucial.

Although several physical–chemical technologies such as adsorption, oxidation by hydrogen peroxide and ozone, and electrolysis have been used for the removal of color from wastewater, these strategies are costly, less efficient or

produce secondary pollution (Ju et al. 2008). Biological treatment is promising mainly due to its eco-friendly, relatively efficient, and security properties (Du et al. 2013). Different groups of microorganisms such as bacteria, for example *Kocuria rosea* (Parshetti et al. 2006), yeast *Saccharomyces cerevisiae* (Jadhav and Govindwar 2006), fungi *Fomes sclerodermeus* (Papinutti and Forchiassin 2004), *Penicillium ochrochloron* (Shedbalkar and Jadhav 2011), and *Coriolopsis* sp. (Chen and Yien Ting 2015) all decolorize MG via biosorption and/or various decolorizing enzymes. In contrast to treatment which uses microorganisms directly, in vitro treatment with cell-free enzymes has many advantages, such as the ability to operate in a wide range of compound concentrations, pH values, temperatures, and salinity without adapting to the biomass, and avoids long incubation processes and biosorption effects. Furthermore, the degradative ability of enzymes may not be affected by toxic compounds which could inhibit cellular systems (Contreras et al. 2012). Therefore, treatment with cell-free enzymes is a simpler and more effective technique (Karam and Nicell 1997).

Manganese peroxidase (MnP, EC 1.11.1.13) is an important extracellular ligninolytic enzyme, and is isolated from many species of white rot fungi, which normally grow on dead wood causing white rot (Tamagawa et al. 2005; Mohammadi and Nasernejad 2009). In the catalytic cycle of heme-containing peroxidase, MnP can catalyze the peroxide-dependent oxidation of Mn^{2+} to Mn^{3+} which is stabilized by organic acids in aqueous solution. The Mn^{3+}–organic acid complex acts as a diffusible redox-mediator that has a low molecular weight and is highly active, which in turn oxidizes a variety of monomeric phenols including dyes as well as phenolic lignin model compounds (Wong 2009). Recently, MnP was shown to degrade triclosan (Inoue et al. 2010) and natural rubber (Nayanashree and Thippeswamy 2015), and decolorize different structural classes of dyes such as the indigo dye, indigo carmine (Li et al. 2015a), the azo dye, Remazol Brilliant Violet 5R, the anthraquinone dye, Remazol Brilliant Blue R, and the triphenylmethane dye, methyl green (Qin et al. 2015). However, few studies have examined the degradation products of dyes and proposed a degradation pathway for catalysis by MnP.

The aim of this study was the development of a decolorization system based on the use of crude MnP from *Irpex lacteus* F17 for the degradation and detoxification of the triphenylmethane dye, MG. Therefore, systematic research was carried out to evaluate the influence of reaction parameters (pH, temperature, MG, Mn^{2+}, hydrogen peroxide (H_2O_2), MnP) on the decolorization efficiency of MG. The kinetics of MG decolorization, the primary metabolic pathway during the degradation process, and the toxic effects of MG before and after MnP treatment using test organisms ranging from prokaryotic bacteria to eukaryotic algae were also investigated.

Materials and methods

Chemicals

MG oxalate ($C_{52}H_{54}N_4O_{12}$, purity 95 %) was purchased from Aladdin Industrial Corporation (Shanghai, China). Figure 1 shows the chemical structure of this dye. Other analytical reagents including veratryl alcohol and 2,2'-azino-bis (3-ethylbenzothiazoline-6-sulfonate) (ABTS) were obtained from Sigma–Aldrich (St. Louis, USA). HPLC-grade ammonium acetate, acetic acid, and acetonitrile were supplied by Merck (Darmstadt, Germany).

MnP production and preparation

MnP was obtained from *Irpex lacteus* F17 which was isolated in our laboratory from a decayed wood chip pile in the vicinity of Hefei, China, and was stored in the China Center for Type Culture Collection (CCTCC AF 2014020). For MnP preparation, *I. lacteus* F17 was cultivated in a solid-state fermentation medium as described previously (Zhao et al. 2015). The cultures were harvested when the maximum MnP activity was detected at 84 h, filtered, centrifuged at 7,500 rpm for 30 min at 4 °C to remove solid-state medium, frozen, defrosted, and the precipitated polysaccharides removed by centrifugation. The supernatant was then concentrated using an ultrafiltration stirred cell apparatus (Model 8400, Millipore Corporation, Billerica, Massachusetts, USA) and a YM10 membrane (molecular cutoff of 10 kDa). The concentrate was used as a crude enzyme preparation for subsequent research. The purified MnP preparation for the decolorization experiments was prepared as described by Zhao et al. (2015).

Enzyme assays

The activities of MnP, lignin peroxidase (LiP), and laccase (Lac) were assayed using the methods described in our previous studies (Zhao et al. 2015). Mn^{2+}, veratryl alcohol, and ABTS were used as the corresponding substrates for MnP, LiP, and Lac oxidation, respectively. One unit of enzyme activity (U) was defined as the amount of enzyme oxidizing

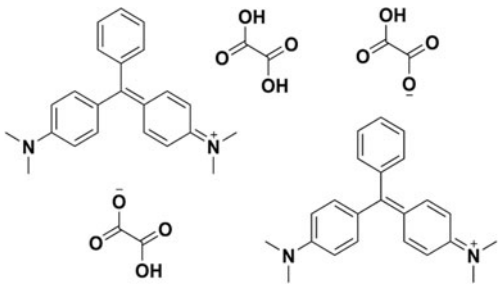

Fig. 1 Chemical structure of MG

1 μmol of substrate per minute. All the enzyme activity assays were carried out at 25 °C and run in triplicate.

Decolorization experiments

Decolorization assays were performed in 50 mM sodium malonate buffer in 15 mL tubes with a 4 mL reaction volume. Various parameters affecting the decolorization of MG were investigated, including pH (3, 3.5, 4, 4.5, 5, 5.5, and 6), temperature (25, 30, 35, 40, 50, 55, 60, and 70 °C), initial dye concentration(100, 200, 250, 300, 400, and 500 mg L^{-1}), $MnSO_4$ concentration (0.1, 0.25, 0.5, 1.0, 2.0, 3.0, and 4.0 mM), H_2O_2 concentration (0.01, 0.025, 0.05, 0.1, 0.15, 0.2, 0.3, and 0.4 mM), and enzyme concentration (11.1, 33.16, 44.22, 66.32, 88.43, and 110.54 U L^{-1}). Controls were prepared with the same amount of heat-inactivated crude enzyme.

The decolorization of MG was measured spectrophotometrically at the absorbance maxima of the dye (λ_{max} = 618 nm) after 1 h of treatment. Each experiment was performed in triplicate. The decolorization percentage was determined as follow:

$$\text{Decolorization}(\%) = \frac{A_0 - A_t}{A_0} \times 100 \quad (1)$$

where A_0 refers to the initial absorbance at 618 nm and A_t refers to the absorbance at 618 nm at reaction time t, respectively.

Enzymatic decolorization kinetics

Determination of the kinetic parameters of MnP

The Michaelis–Menten model equation has been widely used to understand the isothermal kinetics of substrate conversion by enzymes. The Michaelis–Menten constants (K_m and V_{max}) were obtained by linear regression analysis of the double reciprocal Lineweaver–Burk plot (Eq. (2)), using MG as the substrate at various concentrations (50–200 mg L^{-1}).

$$\frac{1}{V_0} = \frac{1}{V_{max}} + \left(\frac{K_m}{V_{max}}\right)\frac{1}{[S]} \quad (2)$$

where S is the MG concentration (in milligram per liter), V_0 is the MG decolorization rate in the first 5 min (in milligram per liter per minute), V_{max} is the maximum MG decolorization rate (in milligram per liter per minute), and K_m is the half-saturation constant (in milligram per liter).

The turnover number (k_{cat} value) was calculated as V_{max}/enzyme protein concentration.

Determination of decolorization reaction order

Under an optimal decolorization system, regression analysis based on the zero-, first-, and second-order reaction kinetics for MG decolorization was conducted. According to the report by Das et al. (2010), the kinetics of MG decolorization can be described by the following equations:

$$C_t = C_0 - k_0 t \quad (3)$$

$$C_t = C_0 e^{-k_1 t} \quad (4)$$

$$\frac{1}{C_t} = \frac{1}{C_0} + k_2 t \quad (5)$$

where C_t is the concentration of MG at reaction time t (in milligram per liter), C_0 is the initial concentration of MG (in milligram per liter), t is the incubation time (in minute), and k_0, k_1, and k_2 are the zero-, first-, and second-order rate constants, respectively.

Degradation analysis

For UV-vis spectral analysis, MG treated with crude MnP at various time periods (0, 5, 10, 15, 20, 25, 30, 40, 50, and 60 min) was scanned at wavelengths ranging from 200 to 700 nm using a UV-vis spectrophotometer (Beckman Coulter DU730, Germany).

For ultra-high performance liquid chromatography (UPLC) and liquid chromatography/time-of-flight/mass spectrometry (LC-TOF-MS) analyses, 20 mL of reaction solution was extracted using dichloromethane, and concentrated to 1 mL. UPLC analysis was performed with an UPLC system (Nexera UPLC LC-30A, Shimadzu, Japan), comprising a Shimadzu Shim-pack XR-ODS III (75 L × 2.0 I.D., 1.6 μm) and a SPD-M20A Prominence diode array detector. The mobile phase was 50:50 (*v*/*v*) acetonitrile: 5 mM ammonium acetate, at a flow rate of 0.3 mL min^{-1}. The detection wavelengths were 618 and 360 nm. MG metabolites were analyzed by LC-TOF-MS (Acquity Ultra Performance LC LCT Premier XE, Waters, Milford, MA, USA) in positive ion mode with a reverse-phase TC C-18 (2) analytical column (250 mm × 4.6 mm I.D., 5 μm, Agilent Technologies, Netherlands). The eluent was 0.2 vol% formic acid in water and acetonitrile (50:50 *v*/*v*), at a flow rate of 1.0 mL min^{-1}.

Ecotoxicity tests

The toxicity of MG before and after treatment was evaluated by two bioassays, which included the bacteria *Escherichia coli* (ATCC 25922), *Proteusbacillus vulgaris* (NICPBP 49027), *Staphylococcus aureus* (ATCC 25923), and *Bacillus subtilis* (ATCC 6633), and the green algae *Chlorella vulgaris* and *Scenedesmus obliquus*. In order to eliminate the effect of

acidic pH on the growth of organisms, the pH values of samples were adjusted to 7.0.

Bacteria toxicity study

A bacteria toxicity study of MG before and after MnP treatment was evaluated by a bacterial growth inhibition test using two gram-negative bacterial strains (*E. coli* and *P. vulgaris*), and two gram-positive bacterial strains (*S. aureus* and *B. subtilis*) according to Palmieri et al. (2005) with slight modifications. Samples (4.5 mL) obtained before and after enzymatic treatment of MG (final concentration of 200 mg L^{-1}) were added to 0.5 mL of 10 × Luria-Bertani (LB) medium, respectively, followed by the addition of bacterial cells (final $OD_{600} = 0.1$) and incubated at 37 °C. Samples withdrawn from each test tube were measured at 600 nm every 2 h for 10 h. A negative control containing nutrient solution only was included for each experiment. The percentage of growth inhibition (GI%) was calculated using the following formula:

$$GI(\%) = \frac{OD_c - OD_s}{OD_c} \times 100 \quad (6)$$

where OD_s is the optical density of the sample at 600 nm and OD_c is the optical density of the control at 600 nm.

Algal toxicity study

Cellular growth of the green algae *C. vulgaris* and *S. obliquus*, which were cultivated in BG11 medium (Feng et al. 2011) was determined. The medium was mixed with the samples of dye solution (final concentration of 100 mg L^{-1}) prior to inoculation of green algal cells (final $OD_{685} = 0.01$) and then incubated for 96 h at 25 °C under an illumination of 3,000 lx with a light/dark cycle of 14: 10 h. The flasks were shaken by hand for 1 min, three times a day, to avoid cell adherence. A negative control containing nutrient solution only was prepared. Algal cell numbers and the maximum absorbance ($\lambda_{max} = 685$ nm) in the visible range are highly correlated (Ma et al. 2002); therefore, the percentage of algal growth inhibition (GI%) was measured at 685 nm using the following formula:

$$GI(\%) = \frac{OD_c - OD_s}{OD_c} \times 100 \quad (7)$$

where OD_s is the optical density of the sample at 685 nm and OD_c is the optical density of the control at 685 nm.

The median effective concentration (EC_{50}) for inhibition of cell growth was also calculated over a 96-h time period using linear regression analysis of transformed MG concentration as natural logarithm data versus percentage growth inhibition to evaluate MG toxicity in the test organisms.

Statistical analysis

The data are reported as mean ± standard deviation. All statistical analyses were carried out using the SPSS v. 15.0 statistical software (SPSS Inc., Chicago, lllinois, USA). Statistical differences between mean values were calculated using one-way analysis of variance (ANOVA). Probability values <0.05 were considered significant.

Results and discussion

Decolorization of MG by MnP

Decolorization of MG by crude enzyme

The crude enzyme solution from *I. lacteus* F17 showed a MnP activity of 923.1 ± 29.5 U L^{-1}, while the activity of LiP and Lac was 28.7 ± 2.8 and 11.9 ± 0.8 U L^{-1}, respectively. To examine the possibility that dye decolorization was due to the role of LiP or Lac, MG decolorization experiments using the crude enzyme were conducted in the absence of Mn^{2+} or both Mn^{2+} and H_2O_2. The decolorization percentage of MG was reduced from 81.9 to 7.7 % in the absence of Mn^{2+} and to 0 % in the absence of both Mn^{2+} and H_2O_2. These results suggested that MnP was the dominant component in the crude enzyme and in the decolorization of MG.

Comparison of MG decolorization by purified and crude MnP

With the decolorization system of 200 mg L^{-1} MG at a pH of 3.5 and a temperature of 40 °C, the decolorization of MG by purified and crude MnP was compared (Fig. 2). Decolorization was 90.3 and 87 % with purified and crude MnP, respectively, following 50-min reaction time. These results indicated that the decolorization of MG was not obviously different between purified and crude MnP. The use of

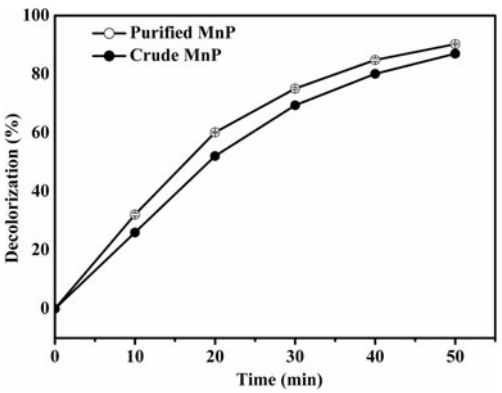

Fig. 2 Comparison of 200 mg L^{-1} of MG decolorized by purified and crude MnP at various time periods. *Error bars* correspond to standard deviation of three samples

purified MnP for decolorization is not applicable on a large scale due to its high cost related to enzyme purification. Thus, crude MnP to decolorize MG may be a good choice, as it is obtained by a simple and low cost preparation process. Therefore, decolorization of MG was further studied using crude MnP from *I. lacteus* F17 and the effects of key factors on dye decolorization were examined.

Effects of key factors on dye decolorization

Effect of pH

To determine the effect of pH on decolorization, the buffer used was 50 mM sodium malonate for pH values between 3 and 6. Figure 3a shows that pH significantly influenced the decolorization of MG by crude MnP, with greatest decolorization (92.1 %) at pH 3.5 after 1-h reaction time. When the pH was set below 3.0, the decolorization efficiency decreased rapidly to 28.5 %. Thus, pH 3.5 was chosen for the decolorization of MG.

In the study conducted by Yu et al. (2006), the optimal pH value was 2.9 for decolorization of the azo dye, reactive brilliant red K-2BP, by crude MnP. Low pH is favorable for MnP decolorization due to the increased redox potential of the oxidized heme (Petruccioli et al. 2009). However, at lower pH, dye decolorization percentage declined sharply, which may have been due to the solvated proton of H_2O_2 forming stable $H_3O_2^+$ presumably resulting in reduced activity of H_2O_2 with the enzyme (Zhang et al. 2012). On the other hand, at higher pH values, H_2O_2 undergoes self-decomposition leading to loss of its oxidation power (Shemer and Linden 2006).

Effect of temperature

The decolorization process was carried out at various temperatures (25, 30, 35, 40, 50, 55, 60, and 70 °C). As seen in Fig. 3b, the decolorization percentage remained high in the range of 35–50 °C and decolorization was optimal (96.4 %) at 40 °C.

The temperature effect on MG decolorization was related to the temperature dependence of enzyme activity. In our previous

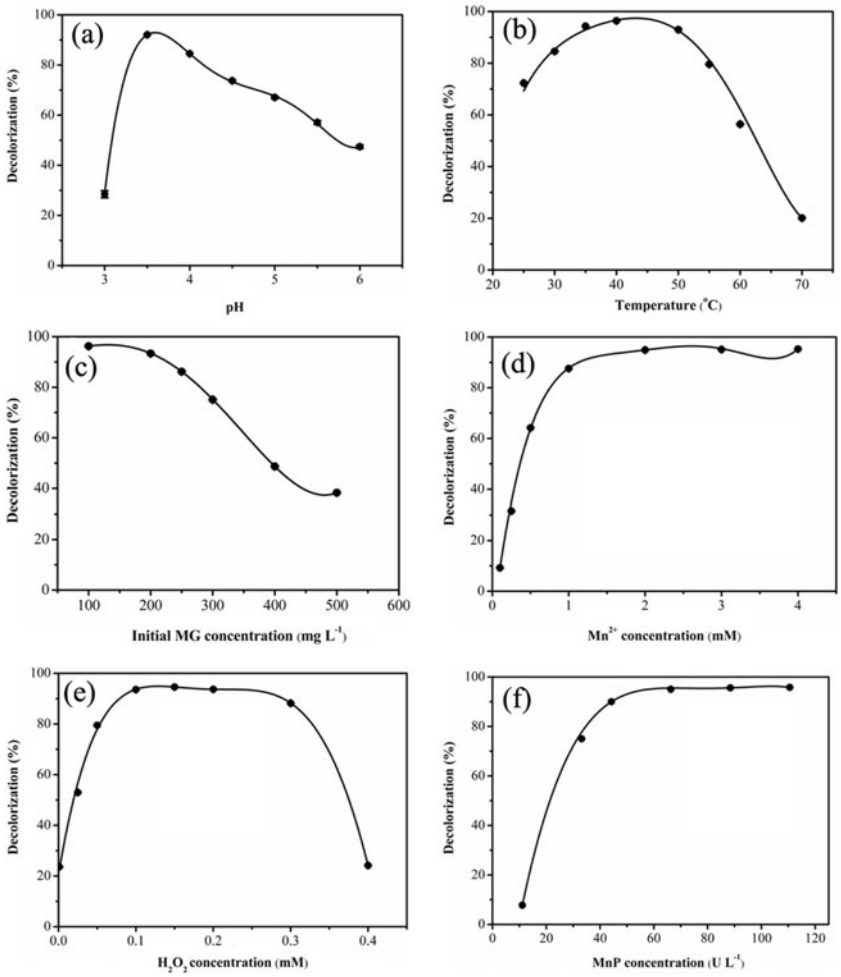

Fig. 3 Influence of **a** pH, **b** temperature, **c** initial MG concentration, **d** Mn^{2+} concentration, **e** H_2O_2 concentration, and **f** MnP concentration on MG decolorization by crude MnP. Experimental conditions: **a** [sodium malonate buffer] = 50 mM, [MG] = 100 mg L^{-1}, [Mn^{2+}] = 1.9 mM, [MnP] = 90.1 U L^{-1}, [H_2O_2] = 0.16 mM, temperature = 35 °C, contact time = 1 h, pH = 3–6; **b** pH = 3.5, temperature = 25–70 °C, and other conditions are same as those of **a**; **c** temperature = 40 °C, [MG] = 100–500 mg L^{-1}, and other conditions are same as those of **b**; **d** [MG] = 200 mg L^{-1}, [Mn^{2+}] = 0.1–4.0 mM, and other conditions are same as those of **c**; **e** [Mn^{2+}] = 2.0 mM, [H_2O_2] = 0.01–0.4 mM, and other conditions are same as those of **d**; **f** [H_2O_2] = 0.1 mM, [MnP] = 11.1–110.54 U L^{-1}, and other conditions are same as those of **e**. *Error bars* correspond to standard deviation of three samples

study (Zhao et al. 2015), MnP from *I. lacteus* F17 was stable and retained its activity at temperatures up to 55 °C. Therefore, at the temperature range of 35–50 °C, the decolorization rate was high due to favorable enzyme-catalyzed reactions.

Effect of initial dye concentration

As shown in Fig. 3c, in the concentration range of 100–200 mg L^{-1} of MG, high decolorization (96.3 to 93.4 %) was observed after 1 h of enzymatic reaction. With increasing MG concentration, i.e., 200–500 mg L^{-1}, a significant decrease (93.4 to 38.3 %) in dye decolorization was observed. To better understand this behavior, decolorization was carried out at MG concentrations of 300 and 400 mg L^{-1}, by increasing the initial amount of MnP, Mn^{2+}, and H_2O_2, respectively, in the decolorization reaction system. The results indicate that the decolorization efficiency of MG increased only with an increasing concentration of H_2O_2 (from 0.1 to 0.2 mM), and was not affected by the addition of MnP or Mn^{2+} (data not shown). Thus, it can be suggested that the low decolorization efficiency could be attributed to the insufficient concentration of H_2O_2 at MG concentrations greater than 300 mg L^{-1}. A case like this has been reported by Yu et al. (2006). Consequently, the MG concentration of 200 mg L^{-1} was the best choice for subsequent decolorization experiments.

Effect of Mn^{2+} concentration

The effect of Mn^{2+} concentration was determined using the range of 0.1–4.0 mM. As seen from Fig. 3d, the decolorization percentage was stable when the concentration of Mn^{2+} reached 2.0 mM, with a maximal MG decolorization of 94.9 %. Thus, a Mn^{2+} concentration of 2.0 mM was optimal for the decolorization of MG at an enzyme concentration of 90.1 U L^{-1}.

Effect of H_2O_2 concentration

The effect of H_2O_2 concentration was studied at values ranging from 0.01 to 0.4 mM when the initial concentration of MG was 200 mg L^{-1}. Figure 3e shows that the decolorization percentage reached 93.6 % in the presence of 0.1 mM H_2O_2 after 1-h reaction time and remained at a high and stable level when the H_2O_2 concentration was between 0.1 and 0.3 mM. Dye decolorization decreased markedly to 24.2 % when the H_2O_2 concentration was 0.4 mM. To ensure both high decolorization efficiency and less consumption of H_2O_2, a H_2O_2 concentration of 0.1 mM was used.

H_2O_2 plays a pivotal role in the catalytic cycle of MnP. Similar results were reported by Yu et al. (2006) who proposed that the greatest decolorization of Reactive brilliant red K-2BP by crude MnP occurred at a H_2O_2 concentration of 0.2 mM and decolorization decreased sharply and was zero with the addition of 0.4 mM H_2O_2. The catalytic cycles of ligninolytic peroxidases consist of a two-electron oxidation of the native ferric enzyme to compound I by H_2O_2 and two single-electron reductions via an intermediate compound II to its resting state by appropriate reduction of substrates (redox mediators or target compounds) (Wen et al. 2010). With excess H_2O_2, compound II is converted to compound III which in turn converts H_2O_2 to a hydroxyl radical. Subsequently, the hydroxyl radical may attack the tetrapyrrol structure of the heme group leading to inactivation of enzymes such as cytochrome P450, horseradish peroxidase, and chloroperoxidase (Torres et al. 2003; Park and Clark 2006).

Effect of enzyme concentration

The effect of enzyme concentration on MG decolorization was studied in the range of 11.1–110.54 U L^{-1}. The relationship between dye decolorization and enzyme concentration is presented in Fig. 3f. The decolorization percentage increased quickly with MnP concentration up to 44.22 U L^{-1}. MG was decolorized to an almost constant level (around 96 %) after 1 h of treatment at MnP concentration values higher than 66.32 U L^{-1}. Thus, it is recommended that enzyme concentration of 66.32 U L^{-1} is used to obtain efficient decolorization.

Effect of reaction time

After optimization of key parameters, the optimal MnP-catalyzed system, including 200 mg L^{-1} MG, 66.32 U L^{-1} crude MnP, 0.1 mM H_2O_2, and 2.0 mM Mn^{2+}, 50 mM sodium malonate (pH 3.5), and a temperature of 40 °C, was very efficient for the decolorization of MG, in which the dye solution rapidly became colorless within the first 1 h (Fig. 4). The decolorization efficiency reached 96 %

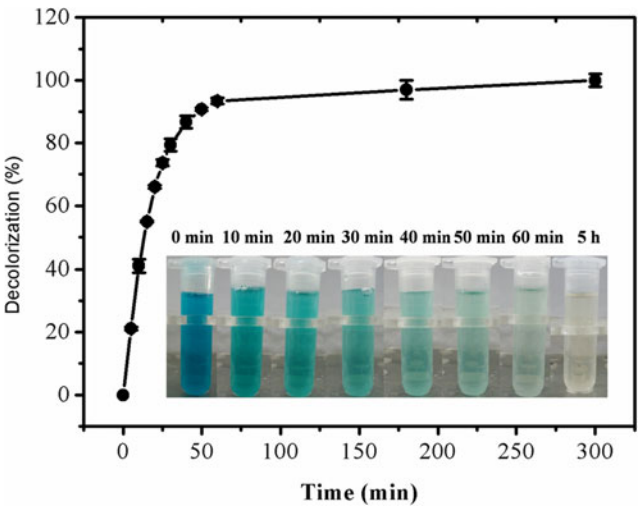

Fig. 4 MnP-catalyzed decolorization of MG under optimal conditions at various time periods and the change in color of MG samples was shown in the inset. *Error bars* correspond to standard deviation of three samples

within 1 h and 100 % within 5 h. MG decolorized by MnP was compared with other reports on MG decolorization. Saravanakumar et al. (2013) reported that 100 mg L^{-1} of MG catalyzed by MnP isozyme H4 was completely decolorized after 6 h. Yang et al. (2015) reported that 91.6 % of 109.9 mg L^{-1} of MG was decolorized when added to 2.8 U mL^{-1} of Lac after 172.4 min of treatment.

Decolorization kinetics

The kinetic constants of MnP-catalyzed MG decolorization under optimal conditions were determined based on the double reciprocal Lineweaver–Burk plots. The constants obtained were $K_m = 109.9$ μmol L^{-1} and $V_{max} = 152.8$ μmol L^{-1} min^{-1}. The k_{cat} value was 44.5 s^{-1}. Furthermore, the catalytic efficiency expressed as k_{cat}/K_m for MG was 404.9 $(mmol)^{-1}$ L s^{-1}. According to the results of Yang et al. (2015), the K_m and k_{cat} values of Lac from white rot fungus *Cerrena* sp. for MG were 781.9 mM and 9.5 s^{-1}, respectively. Hence, the affinity and catalytic efficiency of MnP in our study for MG was superior to that of Lac from *Cerrena* sp. Fig. 5 shows the zero-, first-, and second-order reaction kinetics for MG decolorization under optimal conditions after 1-h reaction time. The results indicated that the kinetic data for decolorization fitted Eq. (4), as R^2 of the model was 0.9849, while it was only 0.7941 and 0.9464 for the zero- and second-order models, respectively. Therefore, the decolorization of MG by crude MnP was well described by the first-order model with the kinetic rate constant of 0.0129 h^{-1}. Similar results were reported by Zhao et al. (2013) where the degradation of MG followed a first-order kinetic model in a photocatalytic reaction at a MG concentration of 20 mg L^{-1}, whereas Kusvuran et al. (2011) and Li et al. (2015b) found that the degradation of MG conformed to pseudo first-order kinetics by using ozonization process and simulated sunlight irradiation treatment for initial MG concentrations of 1.82–0.30 mM and 10 mg L^{-1}, respectively.

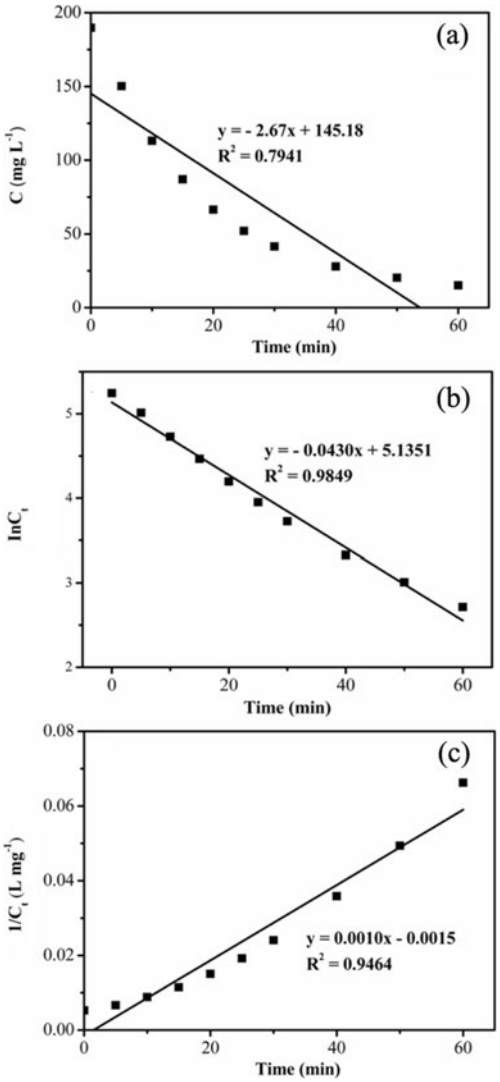

Fig. 5 **a** Zero-, **b** first-, and c second-order reaction kinetics for MG decolorization under optimal conditions after 1 h of treatment

Analysis of possible intermediates of MG degradation by crude MnP

UV-vis spectral analysis

On the basis of the optimization concentration of MG, H_2O_2, Mn^{2+}, and crude MnP, the batch decolorization experiments were conducted at a pH of 3.5 of 50 mM sodium malonate and at a temperature of 40 °C, MG solution before and after decolorization were scanned by a UV–vis spectrophotometer. The results are shown in Fig. 6 and partially enlarged absorption spectra (320–380 nm) are also shown in the inset of Fig. 6. The characteristic peak of MG at 618 nm decreased

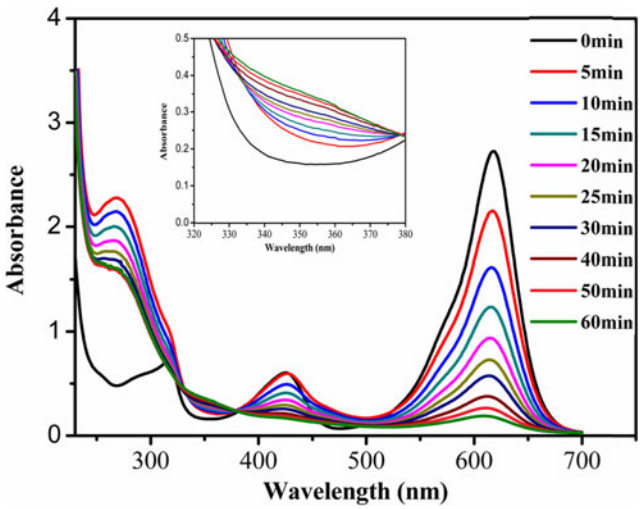

Fig. 6 UV-vis spectral analysis of MG catalyzed by crude MnP at various time periods and the absorption spectra enlarged within 320–380 nm in the inset

gradually over time following decolorization by crude MnP, with a blue-shift of the maximum absorbance peak from 618 to 612 nm. Furthermore, the intensity of the peak at 425 nm decreased, which indicated destruction of the conjugated structure of MG. In contrast, the inset in Fig. 6 shows that the intensity of peaks within 325–375 nm increased. In addition, a significant peak with an absorption maximum at 270 nm was observed. According to previous reports, a complex formed by Mn^{3+} and malonate, with a peak at 270 nm (Boer et al. 2006), was used to oxidize MG. As reported by Murugesan et al. (2009), a blue-shift at approximately 618 nm indicated that the products of N-demethylation of MG had formed, as *N*-demethylation products have maximum absorbance wavelengths lower than those of MG. Moreover, 4-(dimethylamino)benzophenone (DLBP) was one of the main products following an attack on the central carbon atom of MG, with obvious absorbance at 360 nm (Ju et al. 2009).

UPLC analysis

After treatment with crude MnP for 0, 0.5, 1, 3, and 5 h, the intermediates in the aqueous MG solutions were extracted and analyzed by UPLC.

The chromatograms of UPLC recorded at 618 nm are depicted in Fig. S1a. The peak at the retention time (t_R) of 1.576 min was identified as MG which decreased rapidly within 0.5 h and was not detected following incubation for 5 h. A weak peak with $t_R = 1.370$ min was recorded at 618 nm which may have been due to trace impurities. The addition of crude MnP to MG resulted in a decrease in the intensity of this peak. Another weak peak with $t_R = 1.104$ min initially increased and subsequently decreased.

The chromatograms of UPLC recorded at 360 nm are depicted in Fig. S1b, which were used to analyze the products of oxidative cleavage of the C–C double bond in MG. MG was degraded into a series of intermediates with $t_R = 0.926$, 1.320, 1.389, and 2.293 min in UPLC chromatography. A peak was also detected at $t_R = 4.138$ min in the MG control, which was probably due to an impurity.

LC-TOF-MS analysis

Following crude MnP treatment for 0.5 h, the intermediates extracted from aqueous MG solutions were further identified by LC-TOF-MS. The total ion chromatograms are displayed in Fig. S2 and S3, and the main products are shown in Table 1.

According to the results of mass spectral analysis, we assigned the following: (a) $m/z = 301$ as (*p*-methylaminophenyl)(*p*-methylaminophenyl)phenylmethylium (MM-PM); (b) $m/z = 315$ as (*p*-dimethylaminophenyl)(*p*-methylaminophenyl)phenylmethylium (DM-PM); (c) $m/z = 329$ as MG; (d) $m/z = 136$ as dimethyl-(4-oxo-cyclohexa-2,5-dienylidene)-ammonium; (e) $m/z = 150$ as 4-dimethylaminobenzaldehyde; (f) $m/z = 198$ as 4-aminobenzophenone; (g) $m/z = 212$ as 4-(methylamino)-benzophenone; (h) $m/z = 226$ as DLBP. The interesting, but infrequent formation of protonated ions $(M + CH_3CN + H)^+$ was observed for several compounds (d–h). This phenomenon was directly related to the acetonitrile used as mobile phase in LC-MS analysis. Furthermore, after crude MnP treatment for 5 h, MG, DM-PM, and MM-PM were gradually degraded into infinitesimal quantities, and the compounds, DLBP and 4-dimethylaminobenzaldehyde initially increased and subsequently decreased. Also 4-(methylamino)benzophenone increased initially and decreased at 5 h when the abundance of 4-aminobenzophenone sharply increased. In order to further verify these compounds, DLBP and 4-dimethylaminobenzaldehyde were identified with commercially available standards by a HPLC-ESI-MS/MS technique (data not shown). Unlike MG degradation via the bacteria *Shewanella* (Chen et al. 2010), *Pseudomonas aeruginosa* (Kalyani et al. 2012), *Enterobacter asburiae* (Mukherjee and Das 2014), and the fungi *Penicillium pinophilum* and *Myrothecium roridum* (Jasińska et al. 2012), this MnP-catalyzed MG degradation did not detect leucomalachite green (LMG), the reduced form of MG, which is equally toxic

Table 1 Identification of the intermediates of MnP-catalyzed MG degradation by LC-MS

Peaks	Compounds	Rention time (min)	m/z
a	(*p*-Methylaminophenyl)(*p*-methylaminophenyl)phenylmethylium	3.73	301
b	(*p*-Dimethylaminophenyl)(*p*-methylaminophenyl)phenylmethylium	4.13	315
c	MG	4.23	329
d	Dimethyl-(4-oxo-cyclohexa-2,5-dienylidene)-ammonium	5.08	136
e	4-Dimethylaminobenzaldehyde	6.67	150
f	4-Aminobenzophenone	7.28	198
g	4-(Methylamino)benzophenone	10.92	212
h	DLBP	17.29	226

to triphenylmethane dye and was eliminated much slower than the dye itself from the environment (Wu et al. 2011). Therefore, the MnP-catalyzed degradation without the formation of LMG was beneficial in MG detoxification.

Proposed MnP-catalyzed MG degradation pathway

On the basis of the intermediates identified by the above detection methods, the possible pathway of MnP-catalyzed MG degradation is described in Fig. 7.

Given the identification of dimethyl-(4-oxo-cyclohexa-2,5-dienylidene)-ammonium (*m*/*z* 136) and DLBP (*m*/*z* 226) and based on a previous report of ozone treatment of MG (Kusvuran et al. 2011), the degradation in the present study was initiated by oxidative cleavage of the C–C double bond in MG by MnP-generated Mn^{3+}. However, Du et al. (2011) reported that the first step in the biodegradation of MG by *Pseudomonas* sp. strain DY1 under aerobic conditions was hydroxylation to form malachite green carbinol, followed by oxidation and decomposition to *N*,*N*-dimethylaniline and DLBP. Furthermore, Du et al. (2013) found that the degradation of MG by *Micrococcus* sp. strain BD15 began with a hydroxylation process, followed by the cleavage of different C–C bonds of the central carbon to generate either DLBP (*m*/*z* 226) or Michler's ketone. In this study, DLBP (*m*/*z* 226), as one major intermediate production by the MnP-catalyzed was found to undergo two successive N-demethylation steps to 4-(methylamino)benzophenone (*m*/*z* 212) and 4-

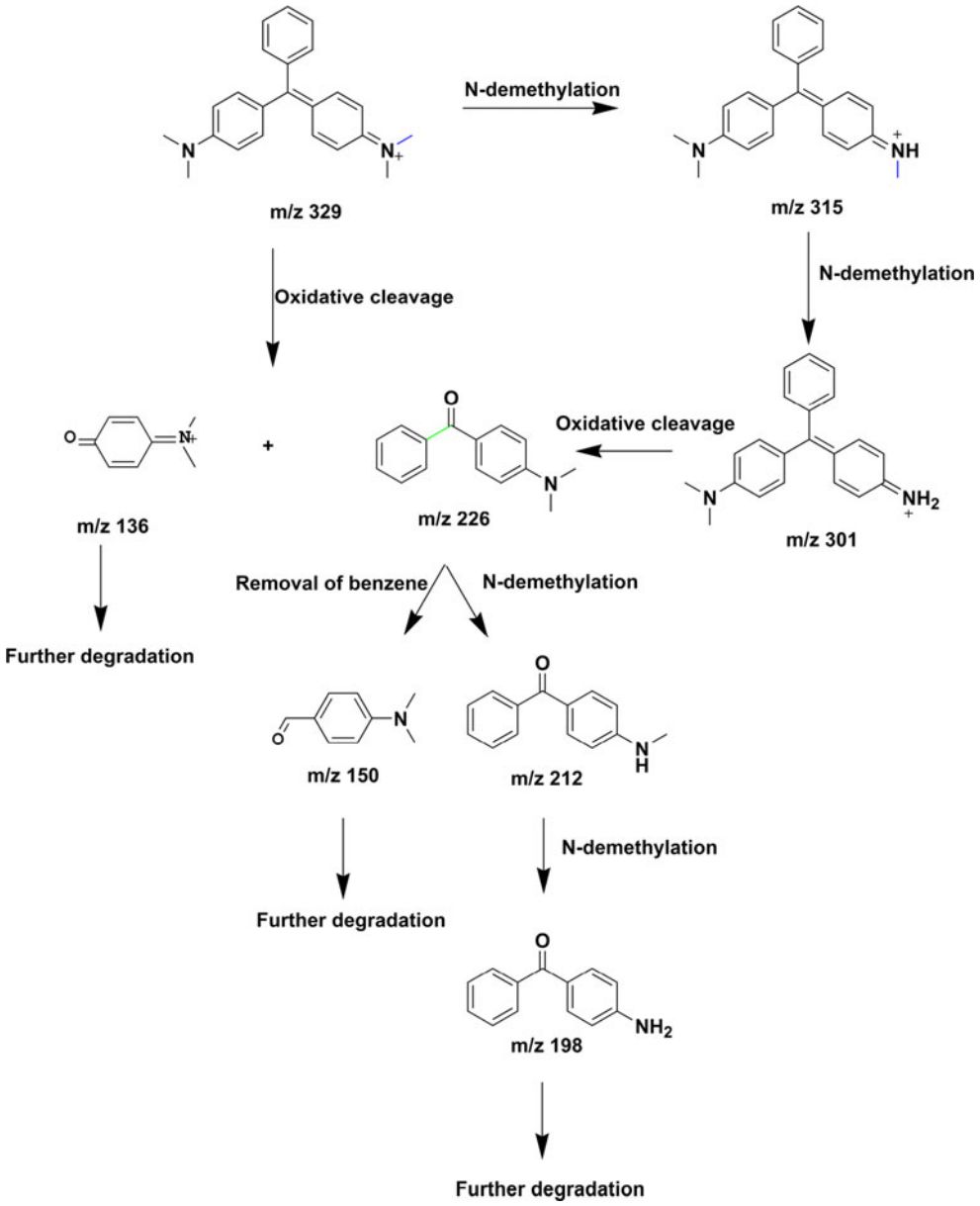

Fig. 7 The proposed MnP-catalyzed MG degradation pathway

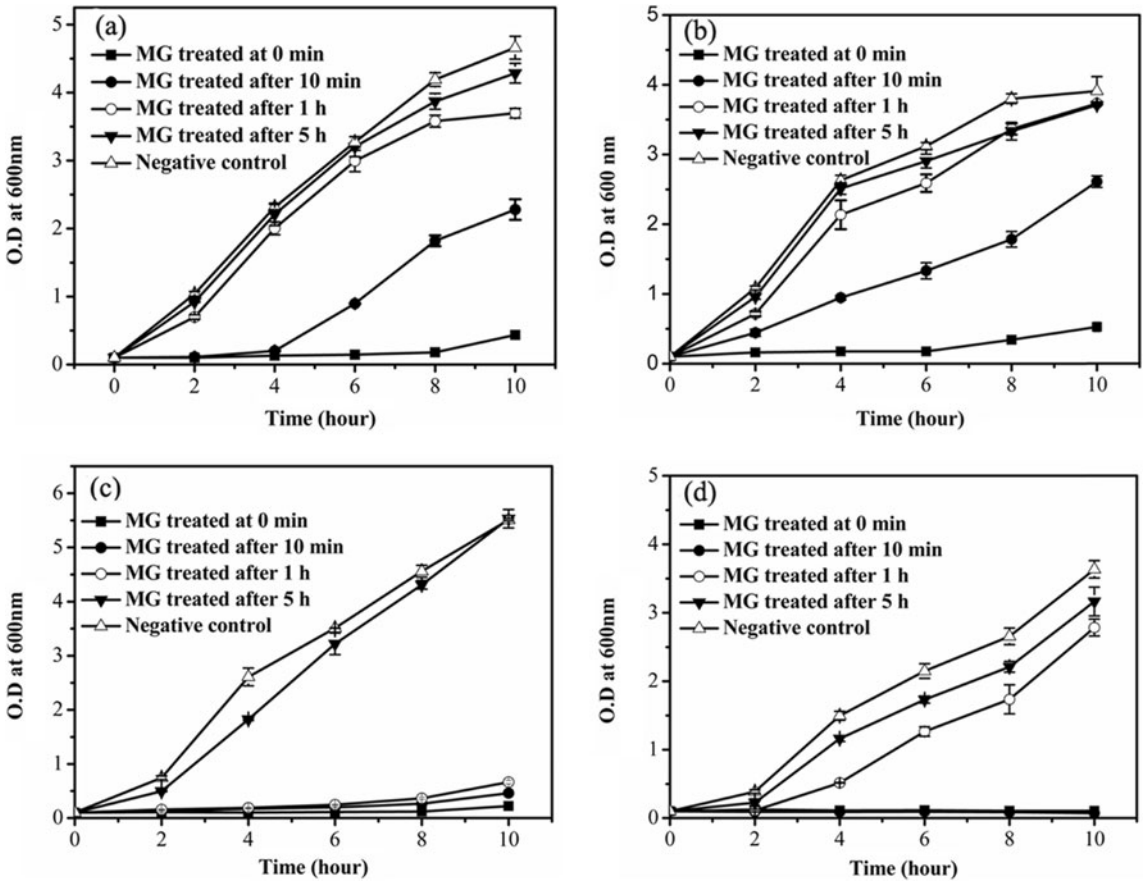

Fig. 8 Bacterial toxicity asssay of a *E. coli*, b *P. vulgaris*, c *S. aureus*, d *B. subtilis* grown in MG and its intermediate products by crude MnP treatment for 0 min, 10 min, 1 h and 5 h during 0-, 2-, 4-, 6-, 8-, and 10-h incubation. *Error bars* correspond to standard deviation of three samples

aminobenzophenone (*m*/*z* 198). DLBP (*m*/*z* 226) was also degraded to 4-dimethylaminobenzaldehyde by the removal of benzene. This is consistent with the study of Yang et al. (2015), who reported that *N*-demethylation of DLBP was observed in a stepwise manner, whereas Du et al. (2013) proposed that DLBP was initially hydroxylated and successively demethylated in a single step.

Given the identification of MM-PM and DM-PM, the degradation could also be initiated by *N*-demethylation of MG. Similarly, Murugesan et al. (2009) proposed that the degradation mediated by Lac started with three successive *N*-demethylation processes of MG, whereas Saravanakumaret et al. (2013) reported that in the degradation of MG by MnP isozyme H4, demethylated products were not detected.

In this study, after 0.5-h treatment, *N*-demethylated products of MG and cleavage products of the conjugated structure of MG were all detected, which indicated that two types of reaction may be two parallel degradation routes in MnP catalyzed MG degradation. The *N*-demethylation and cleavage of the conjugated structure of MG were described as the main pathway in some reports. Cheng et al. (2004) proposed that the degradation of MG started with cleavage of the central carbon, followed by *N*-demethylation during visible light photodegradation in the presence of H_2O_2. Berberidou et al. (2007), in their study of sonolytic, photocatalytic, and sonophotocatalytic reactions of MG, found that parallel and competing pathways between *N*-demethylation reactions and destruction of the conjugated structure.

Table 2 Dose–response relationship of MG to *C. vulgaris* and *S. obliquus*

	Regression equation	Significance level	Correlation coefficient	EC_{50} (mg L^{-1})
C. vulgaris	[a] $P = -233.276 + 102.161 \ln C$	0.010	0.960	16.161
S. obliquus	[a] $P = -204.767 + 80.127 \ln C$	0.000	0.995	24.023

[a] *P* percentage inhibition, *C* MG concentration

It has been confirmed by our earlier study that MnP from *I. lacteus* F17 has the ability to decolorize the polymeric model dye, Poly R-478, and the high redox potential azo dye, Reactive Black 5 (Zhao et al. 2015; Chen et al. 2015). As mentioned above, the MnP-catalyzed reaction is a redox process consisting of the native ferric enzyme as well as the reactive intermediates Compound I and Compound II, thereby forming the catalytic cycle of MnP. The cycle reaction is initiated by binding of H_2O_2 to resting MnP, and then chelates of Mn^{3+} cause one-electron abstraction from the aromatic ring of substrates, producing aryl cation radicals. On the other hand, there was a interaction reaction between chelates of Mn^{3+} and carboxylic acids, which are ultimately converted to alkyl radicals and other radicals. These radicals can attack recalcitrant aromatic structures, giving rise to diverging reactions (Hofrichter 2002). In this study, an efficient reaction system containing MnP from *I. lacteus* F17, sodium malonate, Mn^{2+} and H_2O_2 was found to catalyze C–C double bond cleavage, *N*-demethylation, and C_α-cleavage in the degradation of MG. Thus, it is proposed that the degradation of MG catalyzed by MnP may be via two different routes by either *N*-demethylation of MG or the oxidative cleavage of the C–C double bond in MG. To our knowledge, this study reports for the first time a degradation pathway of MG catalyzed by fungal MnP. Nevertheless, a detailed work is still required to further elucidate the catalytic mechanism of the enzyme.

Toxicity of MG and its degradation products

Bacteria toxicity study

The toxicity of MG (final concentration of 200 mg L^{-1}) and the intermediate products after treatment with MnP for 0 min, 10 min, 1 h, and 5 h was evaluated using *E. coli*, *P. vulgaris*, *S. aureus*, and *B. subtilis*. As seen in Fig. 8, the growth curves of the two gram-negative bacterial strains (*E. coli* and *P. vulgaris*) and the two gram-positive bacterial strains (*S. aureus* and *B. subtilis*) in the control medium and MG after MnP treatment for 0 min, 10 min, 1 h and 5 h showed different slopes. Furthermore, the longer the treatment time, the faster the growth, and the lag phase was shortened. As expected, untreated MG strongly inhibited the growth of *E. coli*, *P. vulgaris*, *S. aureus*, and *B. subtilis* by 90, 86.5, 96, and 100 %, respectively, after a 10-h exposure period, which clearly showed that untreated MG was toxic to the four bacterial strains. Following MG decolorization for 10 min, 1 h, and 5 h, *E. coli* growth inhibition was significantly decreased and was 51.1, 20.7, and 8.0 %, respectively, and *P. vulgaris* growth inhibition was 33.2, 5.1, and 4.6 %, respectively, after a 10-h exposure period. Subsequent to MG enzymatic treatment for 10 min, 1 h, and 5 h, *S. aureus* growth inhibition was decreased and was 91.6, 87.9 and 0 %, respectively, and *B. subtilis* growth inhibition was 98.0, 23.4, and 12.9 %, respectively, after a 10-h exposure period. Variance analysis demonstrated that the reduction in toxicity due to MnP treatment was significant. Chen et al. (2010) reported that the toxicity of MG (100 mg L^{-1}) in *E. coli* decreased slightly after decolorization or extended degradation by *Shewanella decolorationis* NTOU1. Furthermore, Gokulakrishnan et al. (2012) reported that 20 mg L^{-1} of MG after treatment with potassium persulfate for 60 min reduced the growth inhibition by MG in *E. coli.*

Algal toxicity study

The dose–response relationship of MG with both *C. vulgaris* and *S. obliquus*is shown in Table 2. The results showed that the 96 h EC_{50} for *C. vulgaris* and *S. obliquus* was 16.161 and 24.023 mg L^{-1}, respectively. To show the effect of MG treatment with crude MnP on algal growth, growth inhibition of *C. vulgaris* and *S. obliquus* before and after enzymatic treatment was evaluated. The reaction mixture of MG after 5 h of treatment reduced the growth inhibition of *C. vulgaris* and *S. obliquus* by 59.2 and 53.3 %, respectively.

Conclusions

The present study confirmed the decolorization, degradation, and detoxification of MG by crude MnP. The conclusions are summarized as follows:

1. Crude MnP from the white rot fungus, *I lacteus* F17, efficiently decolorized the triphenylmethane dye MG. Under optimal decolorization conditions consisting of 200 mg L^{-1} MG, 66.32 U L^{-1} crude MnP, 0.1 mM H_2O_2, 2.0 mM $MnSO_4$, and 50 mM sodium malonate buffer at a pH of 3.5 and a temperature of 40 °C, the decolorization efficiency was approximately 96 % within 1 h.
2. The kinetics of MG decolorization by crude MnP followed a first-order model. The Michaelis–Menten constants (K_m and V_{max}) and the catalytic efficiency value (k_{cat}/K_m) of MnP for MG were also calculated, which suggested high affinity and high efficiency of the MnP-catalyzed system.
3. Seven intermediates were identified using LC-TOF-MS for MnP-catalyzed MG degradation, in which *N*-demethylation and oxidative cleavage of the C–C double bond of MG was the main degradation mechanism, and a pivotal intermediate, DLBP, decomposed to either 4-(methylamino)benzophenone through one pathway or 4-dimethylaminobenzaldehyde through another pathway.
4. After 5 h of MG decolorization, there was a greater than 90 % decrease in the growth inhibition percentage (GI%) of the two gram-negative and two gram-positive bacterial strains, and a 59.2 and 53.3 % reduction in the green algae *C. vulgaris* and *S. obliquus*, respectively.

Acknowledgements This work was supported by the National Natural Science Foundation of China (31070109, 31570102).

References

Berberidou C, Poulios I, Xekoukoulotakis NP, Mantzavinos D (2007) Sonolytic, photo-catalytic and sonophotocatalytic degradation of malachite green in aqueous solutions. Appl Catal B-Environ 74: 63–72

Boer CG, Obici L, Souza CGMD, Peralta RM (2006) Purification and some properties of Mn peroxidase from *Lentinula edodes*. Process Biochem 41:1203–1207

Chaturvedi V, Bhange K, Bhatt R, Verma P (2013) Biodetoxification of high amounts of malachite green by a multifunctional strain of *Pseudomonas mendocina* and its ability to metabolize dye adsorbed chicken feathers. J Environ Chem Eng 1:1205–1213

Chen C-H, Chang C-F, Liu S-M (2010) Partial degradation mechanisms of malachite green and methyl violet B by *Shewanella* decolorationis NTOU1 under anaerobic conditions. J Hazard Mater 177:281–289

Chen SH, Yien Ting AS (2015) Biodecolorization and biodegradation potential of recalcitrant triphenylmethane dyes by *Coriolopsis* sp. isolated from compost. J Environ Manage 150:274–280

Chen W, Zheng L, Jia R, Wang N (2015) Cloning and expression of a new manganese peroxidase from *Irpex lacteus* F17 and its application in decolorization of reactive black 5. Process Biochem 50:1748–1759

Cheng M, Ma WH, Zhao JC, Huang YP, Zhao JC (2004) Visible-light-assisted degradation of dye pollutants over Fe(III)-loaded resin in the presence of H_2O_2 at neutral pH values. Environ Sci Technol 38: 1569–1575

Clemmensen S, Jensen JC, Jensen NJ, Meyer O, Olsen P, Würtzen G (1984) Toxicological studies on malachite green: a triphenylmethane dye. Arch Toxicol 56:43–45

Contreras E, Urra J, Vásquez C, Palma C (2012) Detoxification of azo dyes mediated by cell-free supernatant culture with manganese-dependent peroxidase activity: effect of Mn^{2+} concentration and H_2O_2 dose. Biotechnol Prog 28:114–120

Das D, Charumathi D, Das N (2010) Combined effects of sugarcane bagasse extract and synthetic dyes on the growth and bioaccumulation properties of *Pichia fermentans* MTCC 189. J Hazard Mater 183:497–505

Du L-N, Wang S, Li G, Wang B, Jia X-M, Zhao Y-H et al (2011) Biodegradation of malachite green by *Pseudomonas* sp. strain DY1 under aerobic condition: characteristics, degradation products, enzyme analysis and phytotoxicity. Ecotoxicology 20:438–446

Du LN, Zhao M, Li G, Xu FC, Chen WH, Zhao YH (2013) Biodegradation of malachite green by *Micrococcus* sp. strain BD15: biodegradation pathway and enzyme analysis. Int Biodeter Biodegr 78:108–116

Feng Y, Li C, Zhang D (2011) Lipid production of *Chlorella vulgaris* cultured in artificial wastewater medium. Bioresource Technol 102: 101–105

Gokulakrishnan S, Parakh P, Prakash H (2012) Degradation of malachite green by potassium persulphate, its enhancement by 1,8-dimethyl-1, 3,6,8,10,13-hexaazacyclotetradecane nickel(II) perchlorate complex, and removal of antibacterial activity. J Hazard Mater 213–214:19–27

Hofrichter M (2002) Review: lignin conversion by manganese peroxidase (MnP). Enzyme Microb Tech 30:454–466

Inoue Y, Hata T, Kawai S, Okamura H, Nishida T (2010) Elimination and detoxification of triclosan by manganese peroxidase from white rot fungus. J Hazard Mater 180:764–767

Jadhav JP, Govindwar SP (2006) Biotransformation of malachite green by *Saccharomyces cerevisiae* MTCC 463. Yeast 23:315–323

Jasińska A, Różalska S, Bernat P, Paraszkiewicz K, Długoński J (2012) Malachite green decolorization by non-basidiomycete filamentous fungi of *Penicillium pinophilum* and *Myrothecium roridum*. Int Biodeter Biodegr 73:33–40

Ju Y, Yang S, Ding Y, Sun C, Gu C, He Z et al (2009) Microwave-enhanced H_2O_2-based process for treating aqueous malachite green solutions: intermediates and degradation mechanism. J Hazard Mater 171:123–132

Ju YM, Yang SG, Ding YC, Sun C, Zhang AQ, Wang LH (2008) Microwave-assisted rapid photocatalytic degradation of malachite green in TiO_2 suspensions: mechanism and pathways. J Phys Chem A 112:11172–11177

Kalyani DC, Telke AA, Surwase SN, Jadhav SB, Lee J-K, Jadhav JP (2012) Effectual decolorization and detoxification of triphenylmethane dye malachite green (MG) by *Pseudomonas aeruginosa* NCIM 2074 and its enzyme system. Clean Techn Environ Policy 14:989–1001

Karam J, Nicell JA (1997) Potential applications of enzymes in waste treatment. J Chem Tech Biotechnol 69:141–153

Kusvuran E, Gulnaz O, Samil A, Yildirim Ö (2011) Decolorization of malachite green, decolorization kinetics and stoichiometry of ozone-malachite green and removal of antibacterial activity with ozonation processes. J Hazard Mater 186:133–143

Li H, Zhang R, Tang L, Zhang J, Mao Z (2015a) Manganese peroxidase production from cassava residue by *Phanerochaete chrysosporium* in solid state fermentation and its decolorization of indigo carmine. Chinese J Chem Eng 23:227–233

Li Y, Gao Z, Ji Y, Hu X, Sun C, Yang S et al (2015b) Photodegradation of malachite green under simulated and natural irradiation: kinetics, products, and pathways. J Hazard Mater 285:127–136

Ma J, Xu L, Wang S, Zheng R, Jin S, Huang S et al (2002) Toxicity of 40 herbicides to the green alga *Chlorella vulgaris*. Ecotox Environ Safe 51:128–132

Mukherjee T, Das M (2014) Degradation of malachite green by *Enterobacter asburiae* strain XJUHX-4TM. Clean – Soil Air Water 42:849–856

Murugesan K, Yang I-H, Kim Y-M, Jeon J-R, Chang Y-S (2009) Enhanced transformation of malachite green by laccase of *Ganoderma lucidum* in the presence of natural phenolic compounds. Appl Microbiol Biotechnol 82:341–350

Mohammadi A, Nasernejad B (2009) Enzymatic degradation of anthracene by the white rot fungus *Phanerochaete chrysosporium* immobilized on sugarcane bagasse. J Hazard Mater 161:534–537

Nayanashree G, Thippeswamy B (2015) Natural rubber degradation by laccase and manganese peroxidase enzymes of *Penicillium chrysogenum*. Int J Environ Sci Technol 12:2665–2672

Palmieri G, Cennamo G, Sannia G (2005) Remazol Brilliant Blue R decolourisation by the fungus *Pleurotus ostreatus* and its oxidative enzymatic system. Enzyme Microb Tech 36:17–24

Papinutti VL, Forchiassin F (2004) Modification of malachite green by *Fomes sclerodermeus* and reduction of toxicity to *Phanerochaete chrysosporium*. FEMS Microbiol Lett 231:205–209

Park J-B, Clark DS (2006) Deactivation mechanisms of chloroperoxidase during biotransformations. Biotechnol Bioeng 93:1190–1195

Parshetti G, Kalme S, Saratale G, Govindwar S (2006) Biodegradation of malachite green by *Kocuria rosea* MTCC 1532. Acta Chim Slov 53: 492–498

Petruccioli M, Frasconi M, Quaratino D, Covino S, Favero G, Mazzei F et al (2009) Kinetic and redox properties of MnP II, a major manganese peroxidase isoenzyme from *Panus tigrinus* CBS 577.79. J Biol Inorg Chem 14:1153–1163

Qin X, Zhang J, Zhang X, Yang Y (2015) Induction, purification and characterization of a novel manganese peroxidase from *Irpex lacteus* CD2 and its application in the decolorization of different types of dye. PLoS One 9, e113282

Saravanakumar T, Palvannan T, Kim D-H, Park S-M (2013) Manganese peroxidase H4 isozyme mediated degradation and detoxification of triarylmethane dye malachite green: optimization of decolorization by response surface methodology. Appl Biochem Biotechnol 171: 1178–1193

Shedbalkar U, Jadhav JP (2011) Detoxification of malachite green and textile industrial effluent by *Penicillium ochrochloron*. Biotechnol Bioproc E 16:196–204

Shemer H, Linden KG (2006) Degradation and by-product formation of diazinon in water during UV and UV/H_2O_2 treatment. J Hazard Mater B 136:553–559

Srivastava S, Sinha R, Roy D (2004) Toxicological effects of malachite green. Aquat Toxicol 66:319–329

Srivastava SJ, Singh ND, Srivastava AK, Sinha R (1995) Acute toxicity of malachite green and its effects on certain blood parameters of a catfish, *Heteropneustes fossilis*. Aquat Toxicol 31:241–247

Tamagawa Y, Hirai H, Kawai S, Nishida T (2005) Removal of estrogenic activity of endocrine-disrupting genistein by ligninolytic enzymes from white rot fungi. FEMS Microbiol Lett 244:93–98

Torres E, Bustos-Jaimes I, Borgne SL (2003) Potential use of oxidative enzymes for the detoxification of organic pollutants. Appl Catal B: Environ 46:1–15

Wen X, Jia Y, Li J (2010) Enzymatic degradation of tetracycline and oxytetracycline by crude manganese peroxidase prepared from *Phanerochaete chrysosporium*. J Hazard Mater 177:924–928

Wong DWS (2009) Structure and action mechanism of ligninolytic enzymes. Appl Biochem Biotechnol 157:174–209

Wu J, Li L, Du H, Jiang L, Zhang Q, Wei Z et al (2011) Biodegradation of leuco derivatives of triphenylmethane dyes by *Sphingomonas* sp. CM9. Biodegradation 22:897–904

Yang J, Yang X, Lin Y, Ng TB, Lin J, Ye X (2015) Laccase-catalyzed decolorization of malachite green: performance optimization and degradation mechanism. PLoS One 10, e0127714

Yu G, Wen X, Li R, Qian Y (2006) In vitro degradation of a reactive azo dye by crude ligninolytic enzymes from nonimmersed liquid culture of *Phanerochaete chrysosporium*. Process Biochem 41:1987–1993

Zhang J, Feng M, Jiang Y, Hu M, Li S, Zhai Q (2012) Efficient decolorization/degradation of aqueous azo dyes using buffered H_2O_2 oxidation catalyzed by a dosage below ppm level of chloroperoxidase. Chem Eng J 191:236–242

Zhao K, Lu Y, Lu N, Zhao Y, Yuan X, Zhang H et al (2013) Design of $H_3PW_{12}O_{40}/TiO_2$ nano-photocatalyst for efficient photocatalysis under simulated sunlight irradiation. Appl Surf Sci 285:616–624

Zhao X, Huang X, Yao J, Zhou Y, Jia R (2015) Fungal growth and manganese peroxidase production in a deep tray solid-state bioreactor, and in vitro decolorization of poly R-478 by MnP. J Microbiol Biotechnol 25:803–813